Linear Rheology of Bis-Urea Functionalized Supramolecular Poly(butylacrylate)s: Part I – Weak Stickers

X Callies, C Fonteneau, C Véchambre, S. Pensec, J.-M. Chenal, Laurent Chazeau, Laurent Bouteiller, G Ducouret, Costantino Creton

Linear Rheology of Bis-Urea Functionalized Supramolecular Poly(butylacrylate)s : Part I – Weak Stickers.

X. Callies[a], C. Fonteneau[b,c], C. Véchambre[d], S. Pensec[b,c], J-M. Chenal[d], L. Chazeau[d]

L. Bouteiller[b,c], G. Ducouret[a], C. Creton[a*],

[a]*Laboratoire SIMM, CNRS, UPMC, ESPCI, 10 rue Vauquelin, Paris, 75005, France*

[b]*Sorbonne Université, UPMC Univ Paris 06, UMR 8232, IPCM, Chimie des Polymères, F-75005 Paris, France*

[c]*CNRS, UMR 8232, IPCM, Chimie des Polymères, F-75005 Paris, France*

[d]*Laboratoire MATEIS, CNRS, INSA Lyon, 7 avenue Jean Capelle, Villeurbanne, 69100, France*

costantino.creton@espci.fr

Abstract

We investigated the linear viscoelastic properties in the melt of a series of nearly monodisperse poly(n-butyl acrylate)(PnBA) chains center-functionalized with a bis-urea sticker group, able to self-associate by quadruple hydrogen bonding. All materials are viscoelastic liquids at 40°C and their Newtonian viscosity varies from 100 to 5000Pa.s. However we show clearly that the viscosity changes non monotonously going through a minimum for a molecular weight (M_n) of 20 kg/mol and a sticker density of 1.1 wt%. We found two regimes: For M_n < 20 kg/mol, the viscosity increases with decreasing M_n, the linear viscoelastic properties change dramatically with temperature, forming a viscoelastic gel at 0°C and flowing at 40°C and the strength of the stickers association controls the size of molecular aggregates. However for M_n > 20 kg/mol, the viscosity increases with M_n, the rheology is controlled by the polymer dynamics and the stickers simply increase the terminal relaxation time relative to unfunctionalized PnBA of the same M_n, as expected from sticky reptation theory. Despite clear evidence of sticker-sticker interactions by FTIR, none of the materials self-assemble at 20°C into structures with a long range order detectable by SAXS.

Introduction

During the last decade, supramolecular chemistry has shown its great potential for various applications in material science, with features such as self-healing[1,2,3], stimuli-responsiveness[4] or mechanical strengthening[5,6]. The supramolecular materials are generally composed of polymer chains or oligomers functionalized by strongly interacting moieties. These moieties, sometimes called "stickers", can associate together by non covalent interactions (hydrogen bonds, ionic, metal coordination…). As recently pointed out by Seiffert and Sprakel[6], two types of supramolecular polymers have been typically investigated: (1) entangled systems of supramolecular main-chain polymers formed by assembly of ditopic monomers and (2) covalent, permanent polymer backbones that can undergo reversible association by the interaction of "sticky" chain segments.

Systems of type 1, sometimes named "living polymers", are subject to reversible, random chain scission and recombination. This strongly affects their rheological properties, which have however mostly been studied in solution[7,8,9,10,11]. The rheological properties of the latter systems (i.e. type 2) have been thoroughly studied, in particular in the melt but with a strong emphasis on polymer chains that bear at least two stickers per chain, in order to allow for an efficient elastic behavior[12,13,14,15,16]. Many experimental and theoretical studies showed that in both cases the presence of these stickers strongly affects the rheological properties. In type 1 systems, the molecular dynamics is usually described by the Cates' model[17] while the mechanism of "sticky reptation" developed by Rubinstein and Semenov[18] is the most used theory for polymers with reversible cross-linkers. However, experimental studies in the melt revealed that the combination of polymer dynamics, sticker dynamics and dynamics of possible aggregated structures makes interpretation of the experimental data very difficult[19,20]. It is therefore essential to systematically characterize the rheology of well-defined model systems where the molecular weight of the polymer, the position of the sticker groups on the chain and the sticker concentration are systematically varied.

Among the possible systems, our group has focused in the past on self-assembly and adhesive properties of polyisobutylene chains bearing a single sticker per chain located in its middle. In solution these chains self-associate into cylindrical structures[21] while in the melt they form highly dynamic structures which show some long range order below 50°C and have very interesting properties as soft adhesives[22].

Motivated by this first study, we now investigate systematically the viscoelasticity of supramolecular center-functionalized linear PnBA chains of different molecular weights (Scheme 1). PnBA is widely used as a base polymer for soft adhesives[23,24] and its molecular weight can be conveniently controlled by Controlled Free Radical Polymerization. In this system an increase in molar mass of the polymer is equivalent to a dilution of the stickers relative to the polymer matrix. Thus, a transition between two kinds of dynamics is expected to occur at a critical molecular weight M_c. Below M_c, the density of stickers should be high enough to allow self-assembly into large aggregates and the rheological properties should be regulated by the scission and relaxation of these aggregates. Beyond M_c, the stickers are dispersed in the PnBA melt and should behave as localized and transient attachment points between chains. In order to identify this transition, we investigated a wide range of molecular weights (5 to 115kg/mol) spanning from chains much shorter to much longer than the critical entanglement molecular weight M_e ($M_e \sim$ 20-30 kg/mol for PnBA[25]).

x = Cl / Br
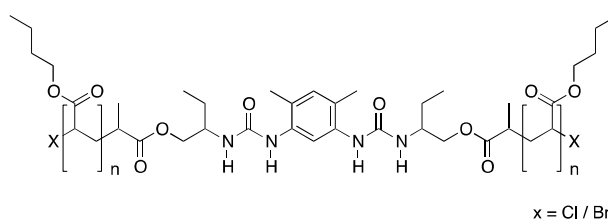
Scheme 1: Structure of the studied PnBA. They were synthesized by ATRP according to Fonteneau et al[26] with molar masses ranging between 5 and 115kg/mol.

The linear rheological properties for this series of bis-urea sticker center-functionalized PnBAs were characterized over a wide range of temperatures (-30°C to 50°C) and the data were analyzed by constructing master curves and by comparing them with those of unfunctionalized PnBA. All these results are then discussed in light of existing models.

Experimental

The polymers were synthesized by ATRP via a functional initiator approach, as reported by Fonteneau et al[26]. The number average molar mass M_n and molar mass distribution Đ (Đ = M_w/M_n with the weight average molar mass M_w) were determined by size exclusion chromatography (SEC) in tetrahydrofuran, with a refractive index detector and a polystyrene calibration curve for samples PnBAX5 and PnBAX8 or with a triple detection set-up for the other samples (see Figure S1 for representative SEC curves). The average degree of polymerization DP and the sticker density Φ_s in the polymer matrix are then estimated: DP = (M_n– M_s)/M_{bu} and Φ_s = M_s/M_n with the molar mass M_s of the sticker and the molar mass M_{bu} of the butylacrylate monomers. The glass transition temperature T_g was determined by DSC with a Q2000 calorimeter (TA Instruments) at a rate of 20°C/min. In order to detect any residual solvent in PnBAX after synthesis, samples are analyzed by NMR H^1 (Bruker Avance 200) (see Figure S2).

Samples	M_n (g/mol)	Đ	DP	Φ_s (wt%)	T_g (°C)
PnBAX5	5400	1.18	38	4.1	-49
PnBAX8	7500	1.23	54	2.9	-47.5
PnBAX20	19800	1.23	150	1.1	-48.7
PnBAX40	43000	1.2	330	0.51	-46.6
PnBAX60	60400	1.22	470	0.36	-48.7
PnBAX115	115000	1.34	890	0.19	-49.4
PnBA107	107000	1.4	840	0	-54.8

Table 1: Characteristics of the samples: number average molar mass M_n, molar mass distribution Đ, sticker density Φ_s in the polymer matrix, average degree of polymerization DP and glass transition temperature T_g.

Dynamic rheological measurements were performed on a stress-controlled rheometer from Anton Paar equipped with a parallel plate geometry (diameter 8.0 or 25 mm, gap 1 to 2 mm). Frequency sweeps (0.02 to 20Hz) were carried out in the linear viscoelastic regime over a large temperature range (50 to -30°C) in order to construct master curves. At the end of the measurements, a frequency sweep is carried out at 25°C to check that the supramolecular structure of PnBAX did not vary during the rheological study, which could last up to 2 days. For all samples, the same frequency dependence of G' and G" at 25°C was observed, as shown in Figure S3 for PnBAX5. PnBAX were also characterized by

thermogravimetric analysis (TGA) to check their thermal stability over the investigated temperature range (see Figure S4) and were found to lose weight only at T > 270°C.

Results

M_n dependence of the viscoelastic properties

Figure 1 shows frequency sweeps performed on bis-urea sticker center-functionalized PnBAs in the linear regime at 20°C. Figure 1a shows the rheological properties of the lower molecular weight polymers and it is clear that, while all three are viscoelastic fluids, the viscosity η^* and terminal relaxation time τ_d, defined as $1/\omega$ at the crossing point between the storage modulus G' and the loss modulus G" increase with decreasing molecular weight. On the contrary Figure 1b shows that for higher molar masses, η^* and τ_d increase with molecular weight (data for PnBAX60 are not shown for clarity but follow a similar trend). Maybe more directly revealing is the value of the complex viscosity η^* at $\omega = 1$ rad/s and T = 20°C as a function of molecular weight or sticker concentration (Figure 2).
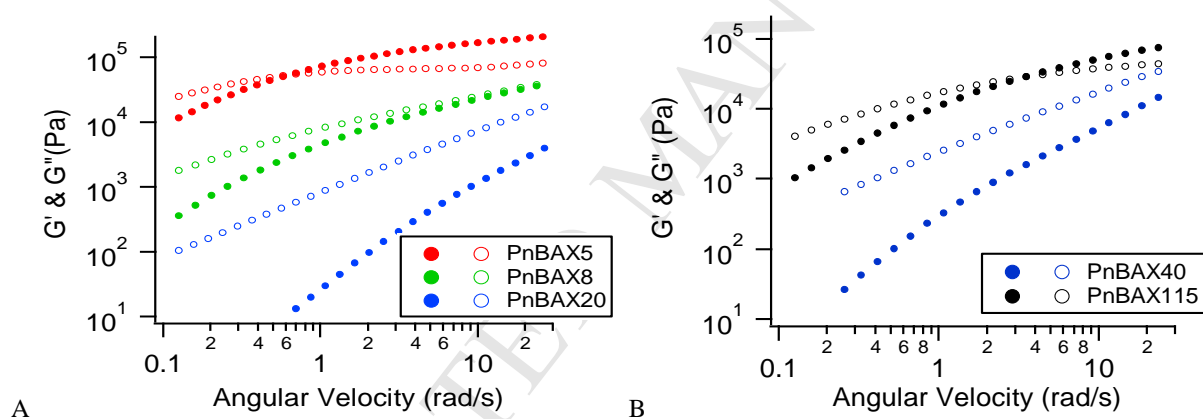

Figure 1: Frequency sweeps at 20°C in the linear regimes for $M_w \leq 20$kg/mol (A) and for $M_w \geq 40$kg/mol (B). G': full symbols; G": hollow symbols.

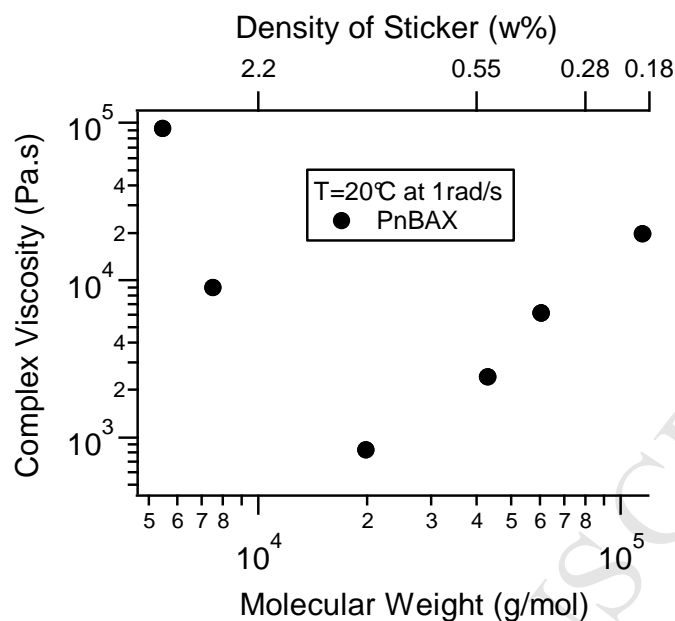Figure 2: Evolution of η*(ω=1rad/s) at 20°C versus M$_w$ or sticker concentration

The results show two regimes with a clear minimum in complex viscosity. Yet the graph is markedly asymmetric. For Mw < 20 kg/mol, the viscosity increases steeply with increasing sticker concentration, while for Mw > 20 kg/mol corresponding to ~1 wt% of stickers the weaker increase in viscosity with increasing molecular weight is due to the increase in molecular size and to the progressive entanglement of the PnBA chains. The asymmetry in behavior is also seen by a quick glance at the temperature dependence of the two materials with the highest and lowest sticker concentration. Figure 3 shows the linear viscoelastic properties of PnBA X5 and PnBAX115 at three different temperatures.
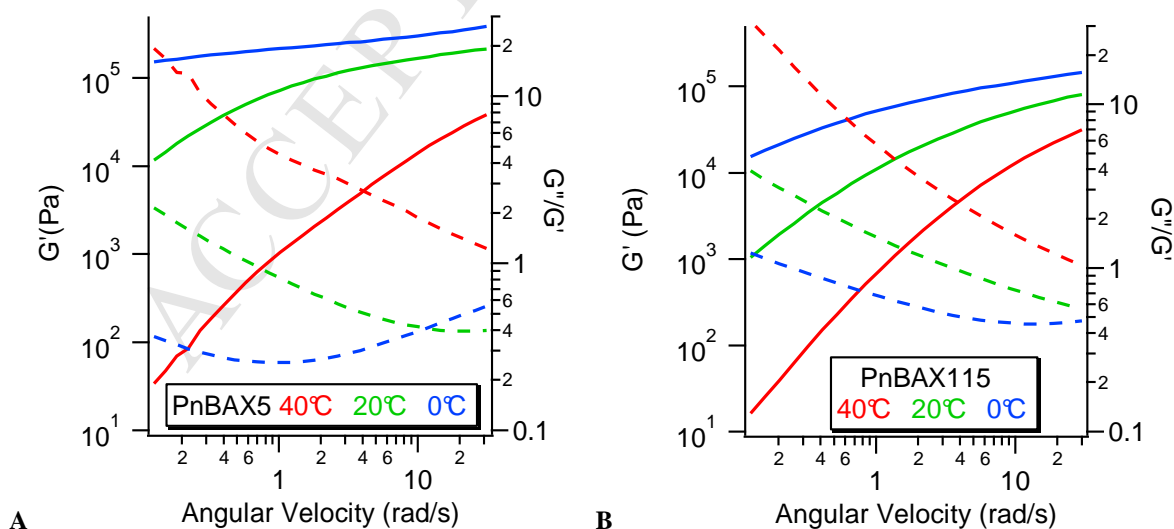

Figure 3: Storage modulus G' and damping factor tan δ = G''/G' as a function of frequency at 0°C, 20°C and 40°C for PnBAX5 (A) and PnBAX115 (B). G': solid line symbols; G''/G': dashed lines.

While for PnBAX115 a horizontal shift clearly leads to a master curve, for PnBAX5 (Figure 3a) the much more pronounced temperature dependence suggests a change in structure.

Master Curves at low Temperature

In linear rheology, the construction of master curves using the time-temperature superposition principle is in principle only possible when the material structure does not depend on temperature. As discussed by Seiffert et al[6], this condition is not easily fulfilled for supramolecular systems which are composed of aggregates or networks assembled by mobile non covalent bonds. However, the successful or unsuccessful construction of such curves is a good probe of molecular dynamics and structure for a given material. In particular, this method was recently used by different authors[27,28,29,30] to identify the sticker contribution to the chain dynamics.

As explained in the Supporting Information (see Figures S5 and S6), horizontal shift factors $a_{(T)}$ are determined by superposing the tan δ curves and then, if this first step works, vertical shift factors $b_{(T)}$ are determined by superposing the G" $(a_{(T)}\omega,T)$ curves. Since the tan δ curves are more sensitive to changes of dynamics or structures in the materials, they will be presented first. The reference temperature $T_{ref}=7°C$ is the minimal temperature for which the superposition of the experimental data works for PnBAX20.

For the two lowest M_n, the superposition of the tan δ (ω, T) curves fails clearly at low temperature in Figure 4. The plot highlights the decrease of the minimum of tan δ in the zone of the elastic plateau (tan $\delta < 1$) and thus, the supramolecular polymers becomes more and more elastic as the temperature decreases. As shown in Figure S7, the superposition of the viscoelastic moduli G' and G" doesn't work either as one would expect.

For $M_n \geq 20kg/mol$, the superposition of the tan δ (ω, T) curves works well for the low temperatures where the elastic plateau is observed over the experimental range of frequencies (see Figure 5). However, the superposition of tan δ (ω, T) curves fails at higher temperatures where these materials are more viscous. Figure 5 highlights that the terminal time τ_d (T_{ref}) of these supramolecular viscoelastic fluids, determined at the end of the elastic plateau by tan $\delta =1$, increases with increasing molecular weight and thus with the length of the side chains. From τ_d $(T_{ref}) = 1/\omega \approx 3.10^{-2}s$ at 20kg/mol, τ_d (T_{ref}) reaches τ_d $(T_{ref}) = 1/\omega \approx 5s$ at 115kg/mol.

The dominant role of the dynamics of the side chains in the rheological response of the material at high M_n is confirmed by the horizontal shifts $a_{(T)}$ displayed in Figure 6. These factors measured for $M_n \geq 20kg/mol$ are surprisingly similar to those obtained for our reference non functionalized PnBA107.
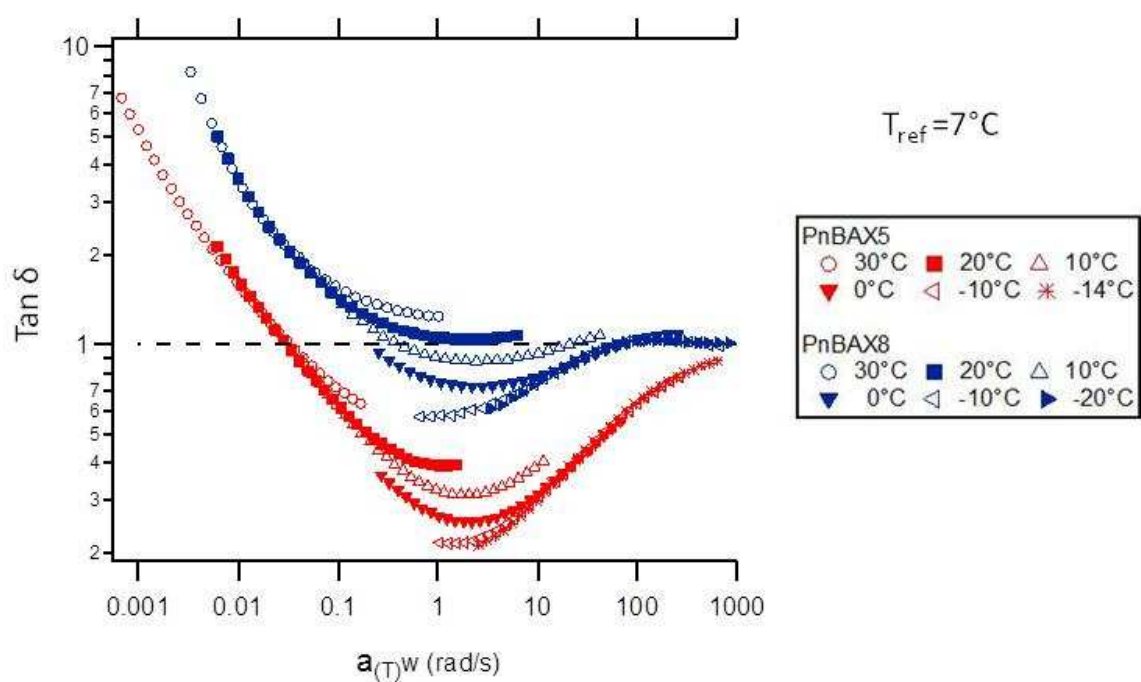
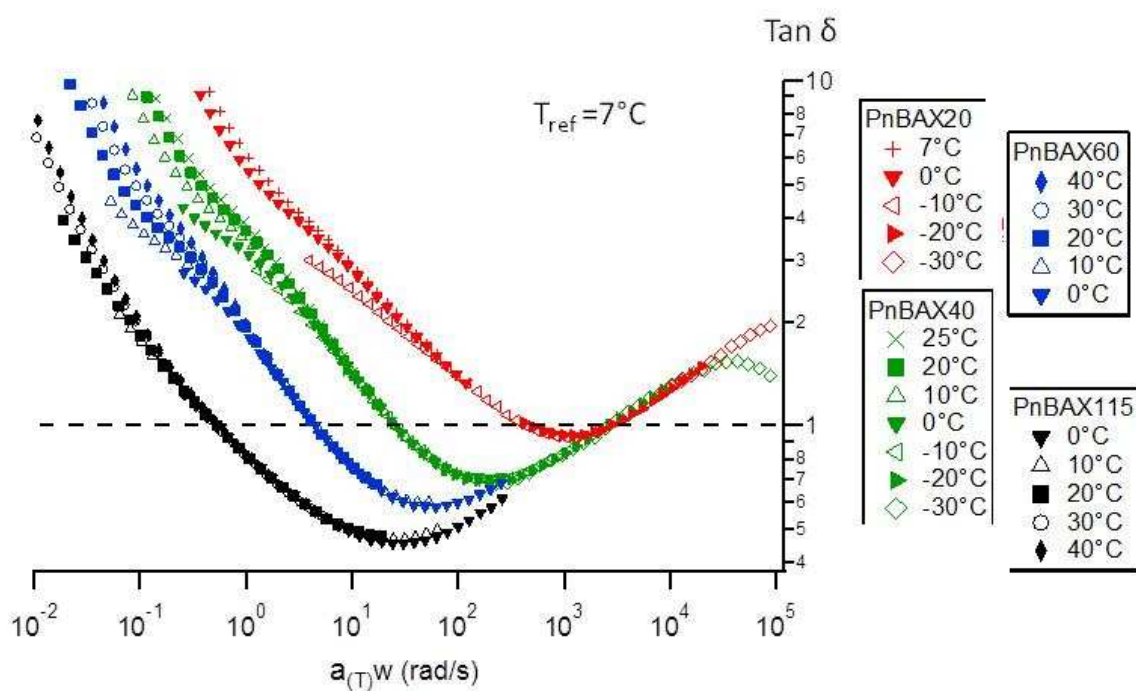Figure 4: Attempts to superpose the tan δ (ω, T) curves for the two lowest M_w. The dashed line (tan δ =1) allows to identify the elastic plateau (tan δ <1).

Figure 5: Attempts to superpose the tan δ (ω, T) curves for $M_w \geq 20$kg/mol. The dashed line (tan δ =1) allows to identify the elastic plateau (tan δ <1).
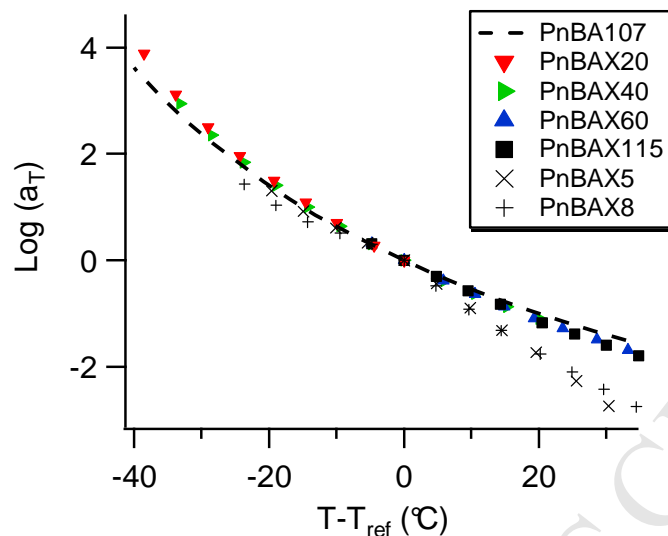
7

Figure 6: Horizontal shifts for the tan δ master curves showed in Figures 4 & 5.

For $M_n \geq 20$kg/mol, G' and G'' master curves provide a snapshot of the viscoelastic properties over a large frequency range at $T_{ref} = 7°C$. As illustrated by PnBAX20 and PnBAX40 in Figure 7, a typical response of lightly entangled polymer is observed for this M_w range: a viscous regime at low $a_{(T)}\omega$ (G'<G''), a viscoelastic part at intermediate $a_{(T)}\omega$ (G'' ≈ G') and then again a dissipative behavior at high $a_{(T)}\omega$. The Figure 7 and S8 show clearly the appearance of an elastic plateau at intermediate $a_{(T)}\omega$ due to the increase of the length of the side chains. The vertical shifts required for the construction of G' and G'' master curves are close to 1 for the investigated temperature range as observed PnBA homopolymers (see Figure S9).
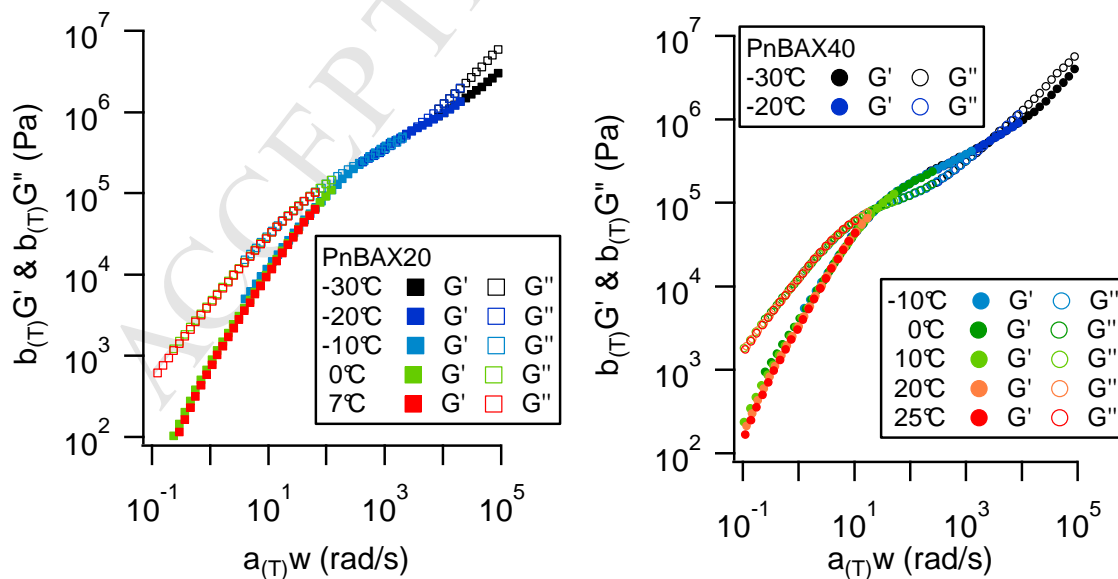

Figure 7: Master Curves for PnBAX20 and PnBAX40 $T_{ref} = 7°C$. G': filled markers; G'': void markers.

Zero-shear Viscosity

While viscoelastic behaviors are observed below room temperature, a liquid-like behavior is observed at higher temperatures for all molecular weights investigated; the viscous modulus G" is always higher than the elastic modulus G' over the experimental range of frequencies at T≥40°C (see Figure S10). The power law exponents at low frequency displayed in Figure S11 are close to what is predicted for a newtonian liquid (G'~ ω^2 & G" ~ ω). As G">10G' in the terminal part of all relaxation spectra, the complex viscosity η^* measured at low frequency (0,1-1rad/s) can be considered as the zero-shear viscosity η_0 by using the empirical Cox-Merz rule: $\eta_0 \approx \lim_{\omega \to 0} (G"/\omega)$ Figure 8 shows the value of the zero-shear rate viscosity obtained in oscillatory shear by using the Cox-Merz rule for all the materials and temperatures where a limiting viscosity was observed. The dependence of η_0 follows the Arrhenius law,

$$\eta_0 = A exp(E_a/RT) \quad (1)$$

with E_a, the activation energy, R the gas constant and A, a prefactor. E_a, which characterizes the temperature dependence of the viscosity η_0, decreases with increasing M_n and approaches the value of E_a measured for non-functionalized PnBA. This decrease of E_a is consistent with the decrease of the density of stickers when M_n increases. However, the remaining difference between the activation energy of PnBAX115 and that of PnBA107 seems to show that the effect of the presence of stickers is not negligible.
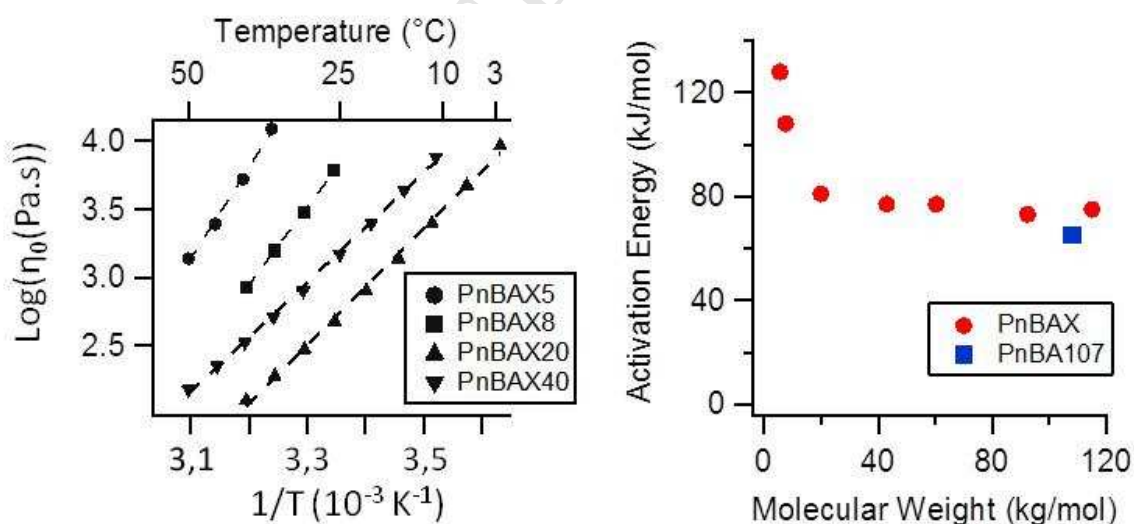

Figure 8: Evolution of η_0 (left) with temperature for Low-M_w PnBAX (Dashed lines are best fits) and variation E_a with the molecular weight and the sticker density (right).

9

Discussion

Over the M_w range from 5.5kg/mol to 115kg/mol PnBAXs flow like liquids while an elastic response is observed at short time scale t < τ_d, with τ_d (T) the terminal time of the supramolecular polymer. The variation of τ_d with M_w at 20°C, shown in Figure 9, highlights the existence of two viscoelastic regimes. To interpret the experimental data it is interesting to compare these experimental values of τ_d with what is expected for unfunctionalized PnBA chains of equivalent molecular weights. Although we did not synthesize PnBA chains for all molecular weights, by using a combination of our experimental data (PnBA107) and a linear viscoelastic model[31,32,25] (see Figures S12 to S15) we can directly compare experimental measurements of the terminal time τ_d (for the functionalized chains) with simulations (for the unfunctionalized ones). Unlike PnBAX and PnBA ($M_n > 2Me$), a crossing point between G' and G" is not observed for PnBA below 2Me. Consequently τ_d is estimated at the minimum of tan δ. As shown in Figure 9, the terminal time of PnBAX is much higher than that of unfunctionalized PnBA in the first regime but tends towards it in the second regime. This comparison shows clearly that the contribution of the side chains becomes increasingly important in the molecular dynamics of the supramolecular material when the molecular weight increases and sticker concentration decreases.
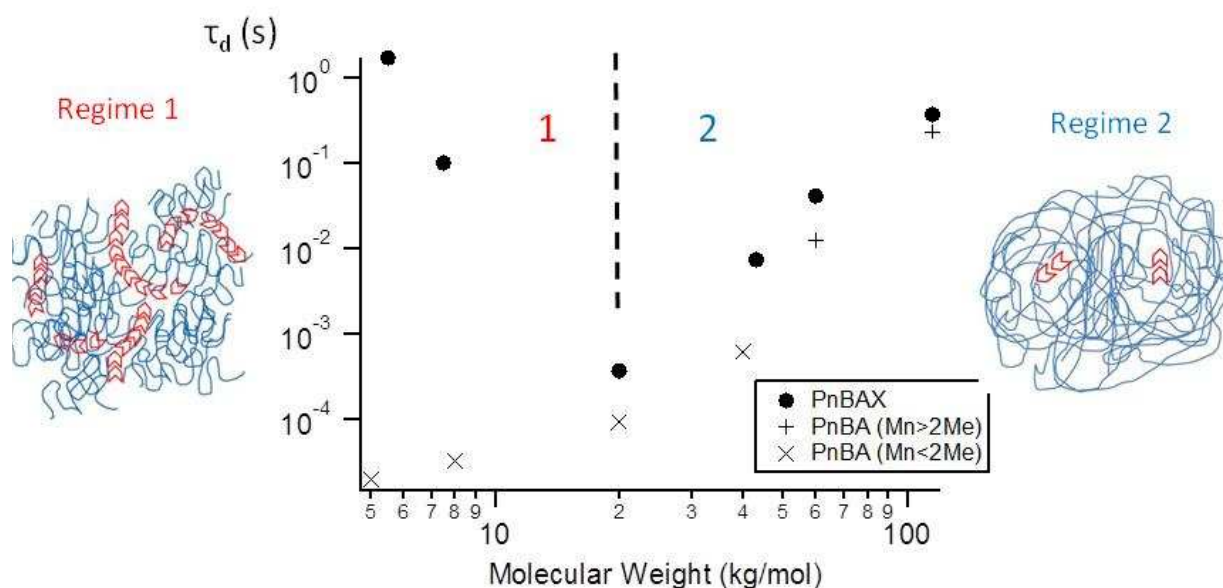

Figure 9: τ_d (T=20°C) vs M_w for PnBAX (circle) and unfunctionalized PnBA (cross). The dashed line materializes the sticker regime at low M_w and the side chains regime at high M_w.

Regime 1: Viscoelasticity regulated by Supramolecular Aggregates

For $M_n \leq 8$kg/mol, the large discrepancy between the terminal times of PnBAX and PnBA as well as the failure to construct proper master curves suggests the existence of supramolecular objects formed by the self-assembly of polar stickers by urea-urea interactions. As the process of self-assembly is fa-

vored by the drop in temperature, an increase in average size of the supramolecular aggregates could explain the increase in elastic character observed at low temperatures in Figure 4. In fact larger objects are more likely to jam and to form a gel than smaller and more mobile objects. On the opposite, when the temperature increases, the scission of aggregates is favored; the average size of such supramolecular aggregates decreases and speeds up diffusion. In addition to the normal decrease in friction coefficient between butylacrylate monomers with increasing temperature, the decrease of the average size of the aggregates could explain the more pronounced temperature dependence of the viscosity η_0 observed for PnBAX than for PnBA (Figure 8). Consequently the terminal time τ_d of these systems can be considered as the longest relaxation time of these supramolecular objects via diffusion or scission process.

To validate this hypothesis, the structure of all samples was investigated in the scale domain of [10 nm-4μm] by small and wide angle X-ray scattering and by AFM at room temperature. Surprisingly and regardless of the molar mass of the PnBAXs, no distinctive peak, characteristic of a self-assembly of the molecules over a long range, was detected (see Figure S16 for WAXS). In addition, the AFM observations did not show any evidence of the presence of supramolecular objects. Nevertheless, FTIR spectroscopy unambiguously showed the presence of inter-urea hydrogen bonding in non polar solution[26]. This suggests that in PnBAX, conversely to previous findings in PIBUT systems, the stickers do not form a supramolecular structure with a long range order. Moreover, if they exist, the supramolecular objects formed by stickers association should be very small, i.e. made of very few associations.

In earlier investigations of our group, the self-assembly and rheology of Ethyl Hexyl bis-Urea Toluene (EHUT), a strongly interacting polar molecule, in a non-polar solvent was extensively studied[33,34]. This small molecule (M_n ~ 400 g/mol), chemically close to our bis-urea sticker, self-assembles into long rods in non polar solvents and the viscoelastic behavior of such solutions was well described by the theory of living polymers[17] proposed by Cates in the fast scission regime. This regime, in which the scission/recombination mechanism is faster than the diffusion of aggregates, is characterized by the Maxwell-like behavior in the terminal part of the relaxation spectrum. Closer to our system, center-functionalized poly(isobutylene) chains self-assemble into comb-shaped aggregates[35,21] in solutions of a non-polar solvent and form a less well-defined structure in the melt[22] with the polymer side chains playing the role of a viscous solvent. These results encouraged us to look for the characteristic rheological signature of worm-like micelles in our PnBAX supramolecular system in the first regime.

The signature of a Maxwellian behavior is the fit of the viscoelastic data by a semi-circle in the Cole-Cole representation (see Figure 10.B). The slight discrepancy observed at high frequency is usually attributed to Rouse-like or breathing mechanisms. As For PnBAX5 and PnBAX8, the superposition of the viscoelastic data with a semi-circle fails clearly at low and high frequency, as shown in Figure 10.A. Therefore, unlike EHUT or worm-like micellar solutions, the molecular dynamics of PnBAX at low M_w cannot be modeled by the fast scission regime of Cates' model. If comb-shaped aggregates exist in PnBAX like in PIBUT, this result suggests that the scission/recombination of stickers is much slower in PnBAX5 than in EHUT solutions, probably due to the presence of the PnBA chains which
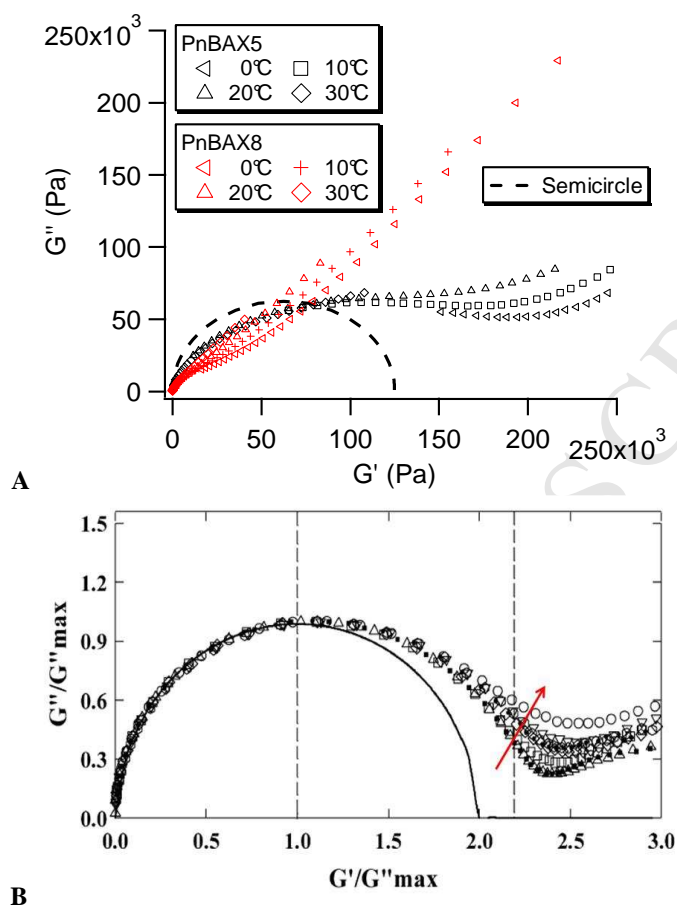
significantly slow down the diffusion of stickers.

Figure 10: Cole-cole plot for PnBAX5 (A) and solutions of EHUT (B) in dodecane (reprinted from reference[34]). The experimental data for PnBAX5 were measured at different temperatures while the experimental measures for EHUT solutions were obtained at different concentrations from c=2.9 to c=10g/L in dodecane, increasing in the direction of the arrow.

Regime 2: Viscoelasticity regulated by PnBA Relaxations

At $M_n \geq 20$kg/mol, the good superposition of the viscoelastic data at high frequency and the similarities of shift factors $a_{(T)}$ with those of pure PnBA suggest that the molecular dynamics of PnBAX is mainly governed by the relaxation of the side chains at short time scales. The terminal time τ_d of these systems, determined by the crossing point between G' and G'' is the longest relaxation time of the side chains. In this M_n range, this relaxation is so dissipative than the scission/recombination dynamics of stickers is only observed at long time scale t >> τ_d. The signature of such scission dynamics is the poor superposition of G' and G'' at low ω in Figure 5 as well as the stronger temperature dependence of the zero shear viscosity η_0 in Figure 8.

Although the characteristic time τ_d is regulated by the relaxation of the side chains beyond 20kg/mol, the comparison between our experimental curves for the PnBAX and the numerical simulations for unfunctionalized PnBA chains in this M_w range shows that the relaxation process at short time scales is still influenced by the presence of stickers. The G' and G'' curves of unfunctionalized poly(butylacrylate) were calculated by using a combination of our experimental data (PnBA107) and a linear viscoelastic model[25] (see Figures S12 to S15). For PnBAXs, a short elastic regime is observed at an intermediate value of ω (tan δ < 1) for all M_n while the behavior remains dissipative for all ω for the unfunctionalized PnBA20 and PnBA40 (see Fig 11.A). The minimum of tan δ is also observed to be lower for PnBAX than pure PnBA (see Figure 11.A or S17) at a fixed molecular weight. The more pronounced elastic character and the higher viscoelastic moduli observed for PnBAX (see Fig 11.B) suggests the presence of small supramolecular aggregates which modify the relaxation of PnBA side chains around them. These small aggregates formed by the self-assembly of stickers would play the role of fillers in the PnBA matrix and would make the materials more elastic. As stickers are expected to self-assemble into comb-shaped aggregates according to our previous studies in solution[21,26], the comparison of our rheological results with numerical models designed for star or comb-shaped poly-mers would be extremely interesting in order to check this hypothesis.
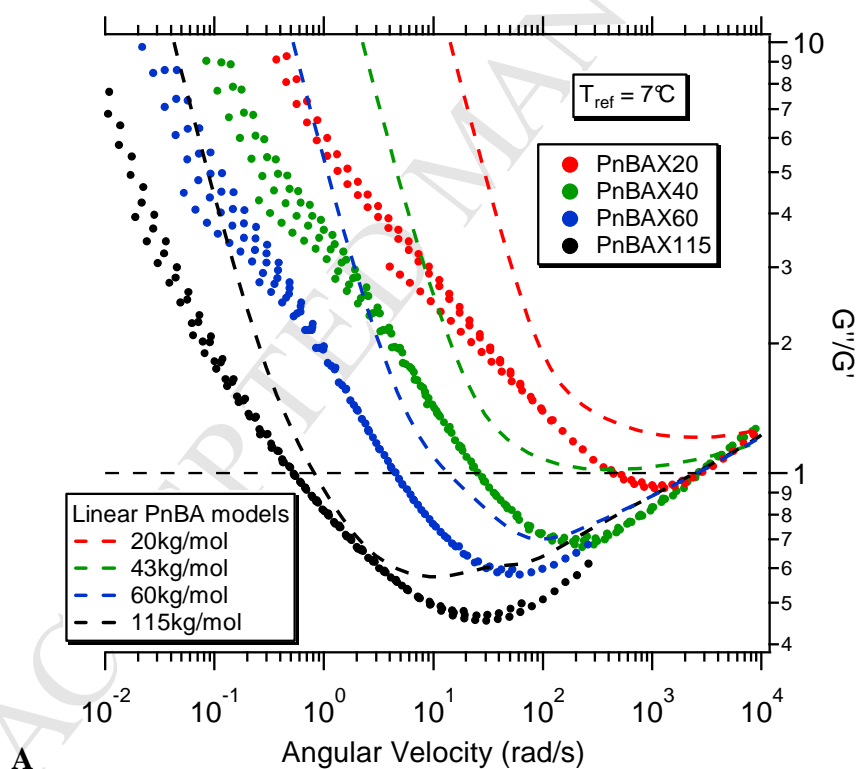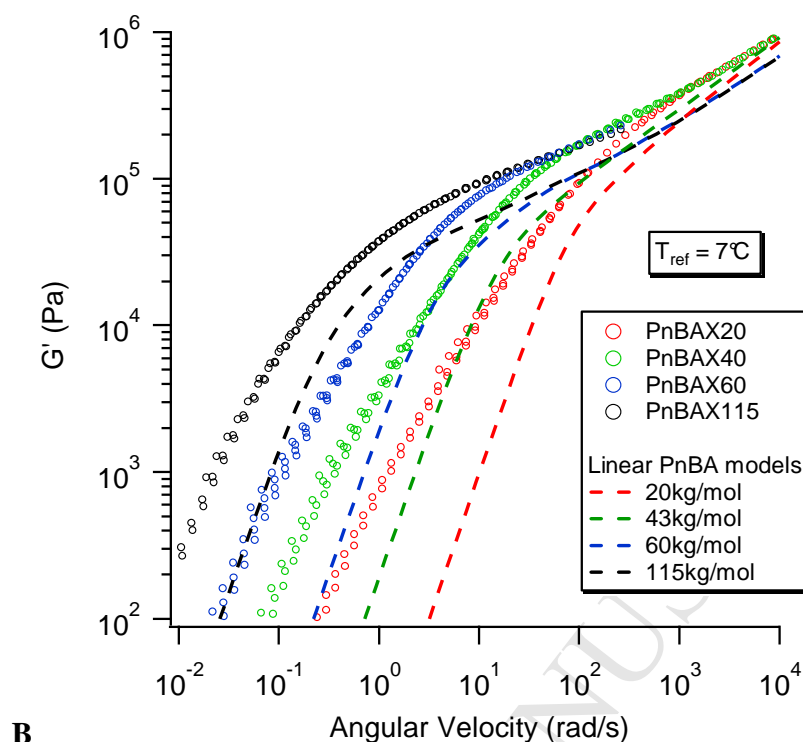
Figure 11: Comparison of our experimental master curves with numerical simulation of monodisperse linear PnBA

Unlike other supramolecular systems described in the literature[28], the change of the molecular dynamics by the stickers is not due to an increase of the glass transition temperature T_g since the same T_g is observed for both regimes (see table 1). Like in the work of Yan et al[29], the analysis of our rheological data by using the time-temperature superposition principle suggests the presence of supramolecular aggregates formed by the self-assembly of bis-urea xylene stickers in the PnBA matrix. However the lack of structure observable by SAXS and AFM would suggest small sizes and no local correlation in orientation for the aggregates.

The qualification of bis-urea as weak stickers may be surprising in view of previous studies on similar studies in apolar solvents or with PIB as the polymer. Yet it is clear that the ester groups on the PnBA compete with the urea groups for hydrogen bonding and weaken the driving force for association of the bis-urea, demonstrating that indeed the definition of strong or weak sticker is completely dependent on the nature of the polymer to which the stickers are attached. Supramolecular systems with similar chain architecture but stronger stickers will be published in a second article. This paper will highlight the role of the strength between stickers on the structure and the rheological properties.

Conclusion

In our study, the linear viscoelastic behavior of an original supramolecular system composed of bis-urea center-functionalized linear and nearly monodisperse PnBA chains was extensively characterized. The synthesis of various samples with well-defined molecular weights with the same sticker reveals a transition between two viscoelastic regimes at a critical molecular weight $M_c \sim 20$ kg/mol. For $M_n <$ M_c the molecular dynamics is regulated by the relaxation of supramolecular aggregates with a random and temperature dependent distribution of sizes. At higher molecular weights, the hydrogen bonding units are diluted in the polymer matrix and the rheological properties become very close to those of unfunctionalized linear PnBA chains but with a longer terminal relaxation time due to sticker/sticker interactions.

References

1. Cordier, P., Tournilhac, F., Soulié-Ziakovic, C. & Leibler, L. Self-healing and thermoreversible rubber from supramolecular assembly. *Nature* **451,** 977–980 (2008).
2. Chen, Y., Kushner, A. M., Williams, G. A. & Guan, Z. Multiphase design of autonomic self-healing thermoplastic elastomers. *Nat. Chem.* **4,** 467–472 (2012).
3. Herbst, F., Döhler, D., Michael, P. & Binder, W. H. Self-Healing Polymers via Supramolecular Forces. *Macromol. Rapid Commun.* **34,** 203–220 (2013).
4. Burnworth, M., Tang, L., Kumpfer, J.R, Duncan, A.J., Beyer, F.L, Fiore, G.L, Rowan, S.J & Weder, C., Optically healable supramolecular polymers. *Nature* **472,** 334–337 (2011).
5. Aida, T., Meijer, E. W. & Stupp, S. I. Functional Supramolecular Polymers. *Science* **335,** 813–817 (2012).
6. Seiffert, S. & Sprakel, J. Physical chemistry of supramolecular polymer networks. *Chem. Soc. Rev.* **41,** 909 (2012).
7. Sijbesma, R. P., Beijer, F. H., Brunsveld, L., Folmer, B. J. B., Hirschberg, J. H. K. K., Lange, R. F. M., Lowe, J. K. L. & Meijer, E. W. Reversible Polymers Formed from Self-Complementary Monomers Using Quadruple Hydrogen Bonding. *Science* **278,** 1601–1604 (1997).
8. Bouteiller, L. in *Hydrogen Bonded Polymers* (ed. Binder, W.) **207,** 79–112 (Springer-Verlag Berlin, 2007).
9. Buhler, E., Candau, S.-J., Kolomiets, E. & Lehn, J.-M. Dynamical properties of semidilute solutions of hydrogen-bonded supramolecular polymers. *Phys. Rev. E* **76,** (2007).
10. Shikata, T., Ogata, D. & Hanabusa, K. Viscoelastic Behavior of Supramolecular Polymeric Systems Consisting of N,N',N''-Tris(3,7-dimethyloctyl)benzene-1,3,5-tricarboxamide and n-Alkanes. *J. Phys. Chem. B* **108,** 508–514 (2004).
11. Yount, W. C., Juwarker, H. & Craig, S. L. Orthogonal Control of Dissociation Dynamics Relative to Thermodynamics in a Main-Chain Reversible Polymer. *J. Am. Chem. Soc.* **125,** 15302–15303 (2003).
12. Folmer, B. J. B., Sijbesma, R. P., Versteegen, R. M., van der Rijt, J. a. J. & Meijer, E. W. Supramolecular polymer materials: Chain extension of telechelic polymers using a reactive hydrogen-bonding synthon. *Adv. Mater.* **12,** 874–878 (2000).
13. Colombani, O., Barioz, C., Bouteiller, L., Chanéac, C;, Fompérie, L., Lortie, F. & Montès, H. , Attempt toward 1D Cross-Linked Thermoplastic Elastomers: Structure and Mechanical Properties of a New System. *Macromolecules* **38,** 1752–1759 (2005).
14. Roosma, J., Mes, T., Leclère, P., Palmans, A. R. A. & Meijer, E. W. Supramolecular Materials from Benzene-1,3,5-tricarboxamide-Based Nanorods. *J. Am. Chem. Soc.* **130,** 1120–1121 (2008).
15. Sivakova, S., Bohnsack, D. A., Mackay, M. E., Suwanmala, P. & Rowan, S. J. Utilization of a Combination of Weak Hydrogen-Bonding Interactions and Phase Segregation to Yield Highly Thermosensitive Supramolecular Polymers. *J. Am. Chem. Soc.* **127,** 18202–18211 (2005).
16. Zhang, R., Yan, T., Lechner, B.D, Schröter, K., Liang, Y., Li, B., Furtado, F., Sun, P. & Saalwächter, K., Heterogeneity, Segmental and Hydrogen Bond Dynamics, and Aging of Supramolecular Self-Healing Rubber. *Macromolecules* **46,** 1841–1850 (2013).

17. Cates, M. E. Reptation of living polymers: dynamics of entangled polymers in the presence of reversible chain-scission reactions. *Macromolecules* **20,** 2289–2296 (1987).
18. Rubinstein, M. & Semenov, A. N. Dynamics of Entangled Solutions of Associating Polymers. *Macromolecules* **34,** 1058–1068 (2001).
19. Herbst, F. & Binder, W. H. Comparing solution and melt-state association of hydrogen bonds in supramolecular polymers. *Polym. Chem.* **4,** 3602–3609 (2013).
20. Herbst, F., Schröter, K., Gunkel, I., Gröger, S., Thurn-Albrecht, T., Balbach, J & Binder, W.H.,. Aggregation and Chain Dynamics in Supramolecular Polymers by Dynamic Rheology: Cluster Formation and Self-Aggregation. *Macromolecules* **43,** 10006–10016 (2010).
21. Pensec, S., Nouvel, N., Guilleman, A., Creton, C., Boué, F. & Bouteiller, L. , Self-Assembly in Solution of a Reversible Comb-Shaped Supramolecular Polymer. *Macromolecules* **43,** 2529–2534 (2010).
22. Courtois, J., Baroudi, I., Nouvel, N., Degrandi, E., Pensec, S., Ducouret, G., Chaneac, C., Bouteiller, L. & Creton, C. , Supramolecular Soft Adhesive Materials. *Adv. Funct. Mater.* **20,** 1803–1811 (2010).
23. Creton, C. Pressure-sensitive adhesives: An introductory course. *Mrs Bull.* **28,** 434–439 (2003).
24. Lindner, A., Lestriez, A., Mariot, S., Creton, C., Maevis, T., Luhmann, B. & Brummer., R. ,Adhesive and rheological properties of lightly crosslinked model acrylic networks. *J. Adhes.* **82,** 267–310 (2006).
25. Jullian, N., Leonardi, F., Grassl, B., Peyrelasse, J. & Derail, C. Rheological Characterization and Molecular Modeling of Poly(n-Butyl Acrylate). *Appl. Rheol.* **20,** 33685 (2010).
26. Fonteneau, C., Pensec, S. & Bouteiller, L. Versatile synthesis of reversible comb-shaped supramolecular polymers. *Polym. Chem.* **5,** 2496 (2014).
27. Feldman, K. E., Kade, M. J., Meijer, E. W., Hawker, C. J. & Kramer, E. J. Model Transient Networks from Strongly Hydrogen-Bonded Polymers. *Macromolecules* **42,** 9072–9081 (2009).
28. Lewis, C. L., Stewart, K. & Anthamatten, M. The Influence of Hydrogen Bonding Side-Groups on Viscoelastic Behavior of Linear and Network Polymers. *Macromolecules* **47,** 729–740 (2014).
29. Yan, T., Schröter, K., Herbst, F., Binder, W. H. & Thurn-Albrecht, T. Nanostructure and Rheology of Hydrogen-Bonding Telechelic Polymers in the Melt: From Micellar Liquids and Solids to Supramolecular Gels. *Macromolecules* **47,** 2122–2130 (2014).
30. Stadler, F. J., Pyckhout-Hintzen, W., Schumers, J.M., Fustin, C.A., Gohy, J.F. & Bailly, C., Linear Viscoelastic Rheology of Moderately Entangled Telechelic Polybutadiene Temporary Networks. *Macromolecules* **42,** 6181–6192 (2009).
31. Majeste, J. C., Montfort, J. P., Allal, A. & Marin, G. Viscoelasticity of low molecular weight polymers and the transition to the entangled regime. *Rheol. Acta* **37,** 486–499 (1998).
32. Léonardi, F., Majesté, J.-C., Allal, A. & Marin, G. Rheological models based on the double reptation mixing rule: The effects of a polydisperse environment. *J. Rheol.* **44,** 675 (2000).
33. Knoben, W., Besseling, N. A. M., Bouteiller, L. & Cohen Stuart, M. A. Dynamics of reversible supramolecular polymers: Independent determination of the dependence of linear viscoelasticity on concentration and chain length by using chain stoppers. *Phys. Chem. Chem. Phys.* **7,** 2390 (2005).
34. Ducouret, G., Chassenieux, C., Martins, S., Lequeux, F. & Bouteiller, L. Rheological characterisation of bis-urea based viscoelastic solutions in an apolar solvent. *J. Colloid Interface Sci.* **310,** 624–629 (2007).
35. Catrouillet, S., Fonteneau, C., Bouteiller, L., Delorme, N., Nicol, E., Nicolai, T., Pensec, S. & Colombani, O., Competition Between Steric Hindrance and Hydrogen Bonding in the Formation of Supramolecular Bottle Brush Polymers. *Macromolecules* **46,** 7911–7919 (2013).
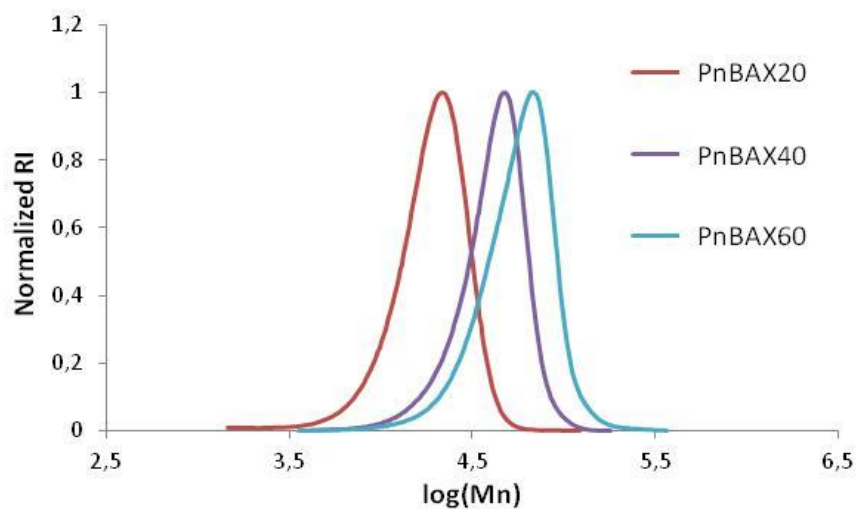
Supporting Information

1. Representative SEC curves

Figure S1: Size exclusion chromatograms of PnBAX20 , PnBAX40 and PnBAX60 (refractive index detection)

2. Nuclear Magnetic Resonance (NMR) Analysis

After synthesis, PnBAX are purified in ethyl acetate. In order to detect any residual solvent in PnBAX, samples were dissolved $CDCl_3$ and then, characterized by NMRH[1] (Bruker Avance 200). As shown in the Figure S2, the characteristic singlet of ethylacetate at 2.05ppm is not observed and thus, no residual solvent seems to remain in our sample when they are characterized in linear rheology.
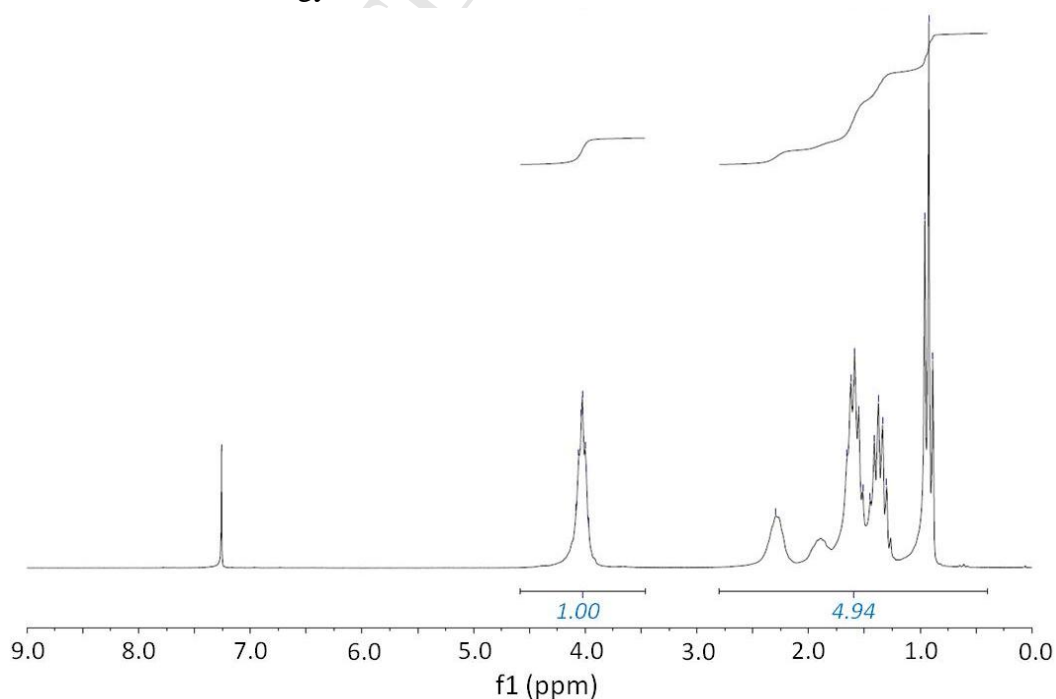
Figure S2: NMR Analysis of PnBAX40 carried out in $CDCl_3$ after synthesis.

RMN 1H (200 MHz, CDCl₃) d (ppm) : 0.89 (t, (CH3-CH2-)n), 1.3 (m, (CH3-CH2-)n), 1.51 (m, (CH3-CH2-CH2)n), 1.77 (br, (CH2-CH-COO)n), 2.2 (br, (CH2-CH-COO)n), 3.99 (br, (CH2-O)n), 7.2 (s, 1H, Ph-H).

3. Stability of PnBAX during the rheological process

At the end of the measurements, a frequency sweep is carried out at 25°C to check the good stability of PnBAX during the rheological analysis, which could last up to 2 days. For all samples, the same frequency dependence of G' and G" at 25°C was observed, as shown in Figure S3 for PnBAX5.
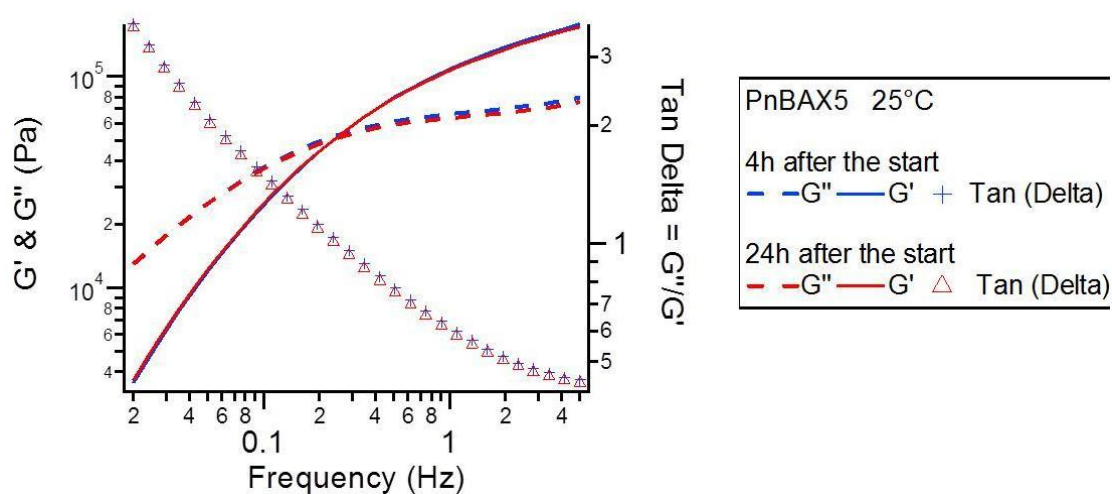
Figure S3: Frequency sweeps achieved at the beginning and at the end of experimental process for PnBAX5.

4. Thermogravimetric Analysis (TGA)

PnBAX were characterized by thermogravimetric analysis (TGA) in order to check if these materials were stable over the investigated temperature range in the rheological study. As illustrated with PnBAX60 in Figure S4, degradation of PnBAX occurs at temperature T ≈ 270°C.

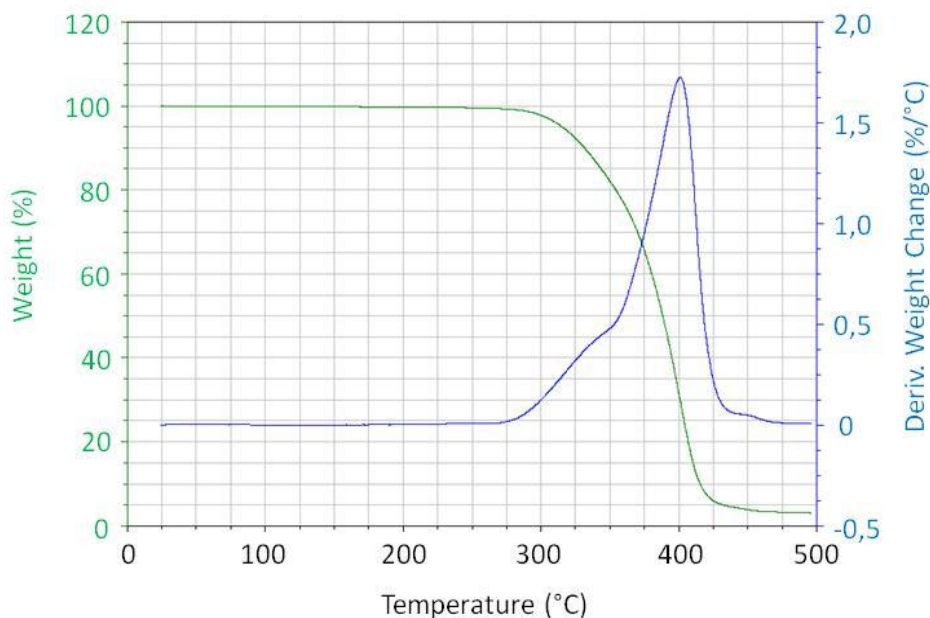Figure S4: Thermogravimetric analysis of PnBAX60, evolution of the weight (%) with temperature (temperature ramp 20°C/min)

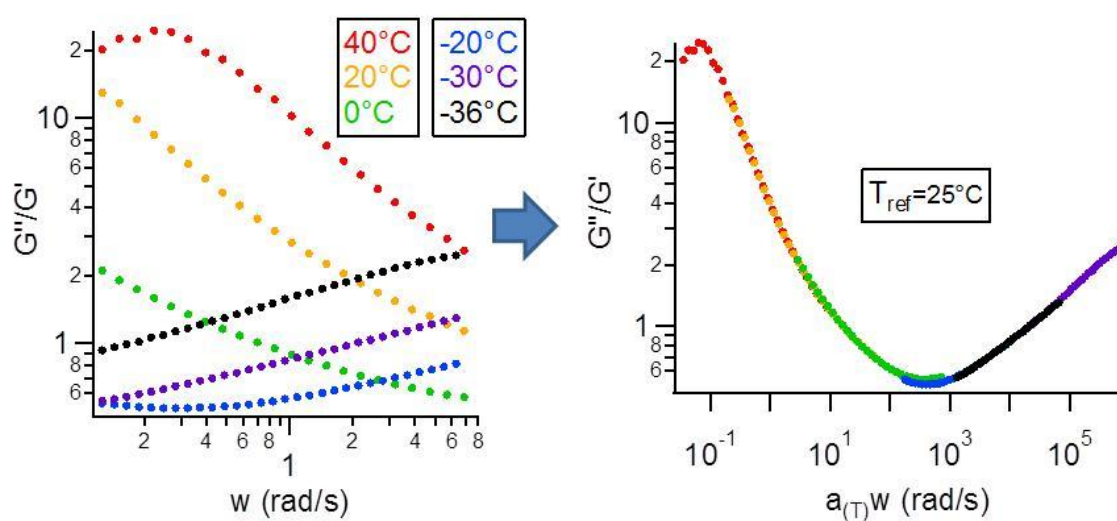# 5. Construction of Master Curves – Data Treatment

Figure S5: Step 1 of the construction of G' and G'' master curves: calculation of horizontal shifts $a_{(T)}$ by superposition of $\tan \delta = G''/G'$ curves.

Master curves are built by superposition of frequency sweeps of G'(ω) and G''(ω) in the linear regime over a large temperature range. An example of such construction is shown in Figure S5 and S6. The curves in these figures were obtained by characterizing a poly(butylacrylate) homopolymer ($M_n = 107$ kg/mol, $I_p = 1,4$).

The horizontal shifts $a_{(T)}$ were calculated by superposing the measures of $\tan\delta\,(\omega,\,T) = G''(\omega,\,T)/G'(\omega,\,T)$ in a first step (see Figure S5) and the vertical shifts $b_{(T)}$ were calculated by superposing $G''(a_{(T)}\omega,\,T_{ref})$ in a second step (see Figure S6).
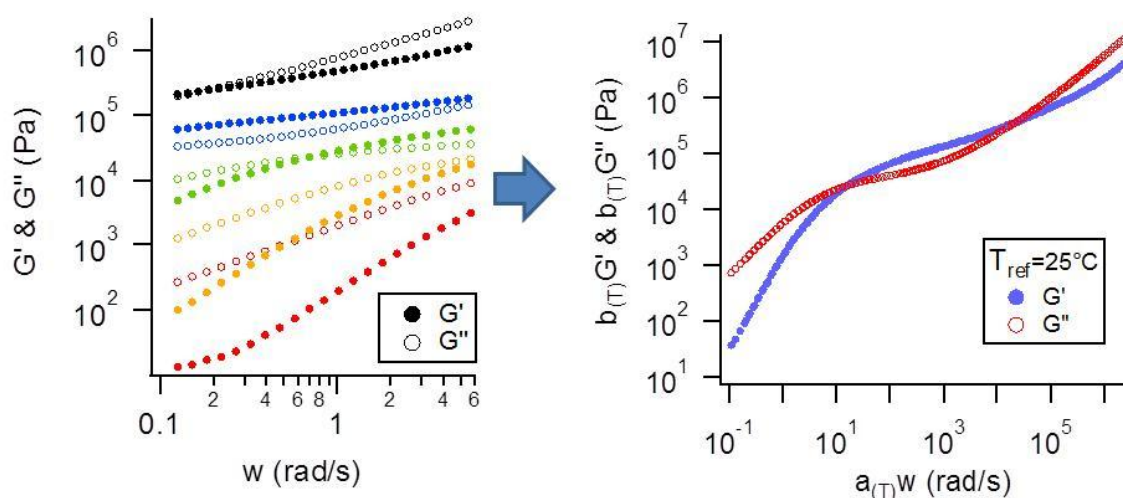

Figure S6: Step 2 of the construction of G' and G'' master curves: calculation of vertical shifts $b_{(T)}$ by superposition of G'' curves after applying $a_{(T)}$.

6. Master Curves – PnBAX at $T_{ref} = 7°C$

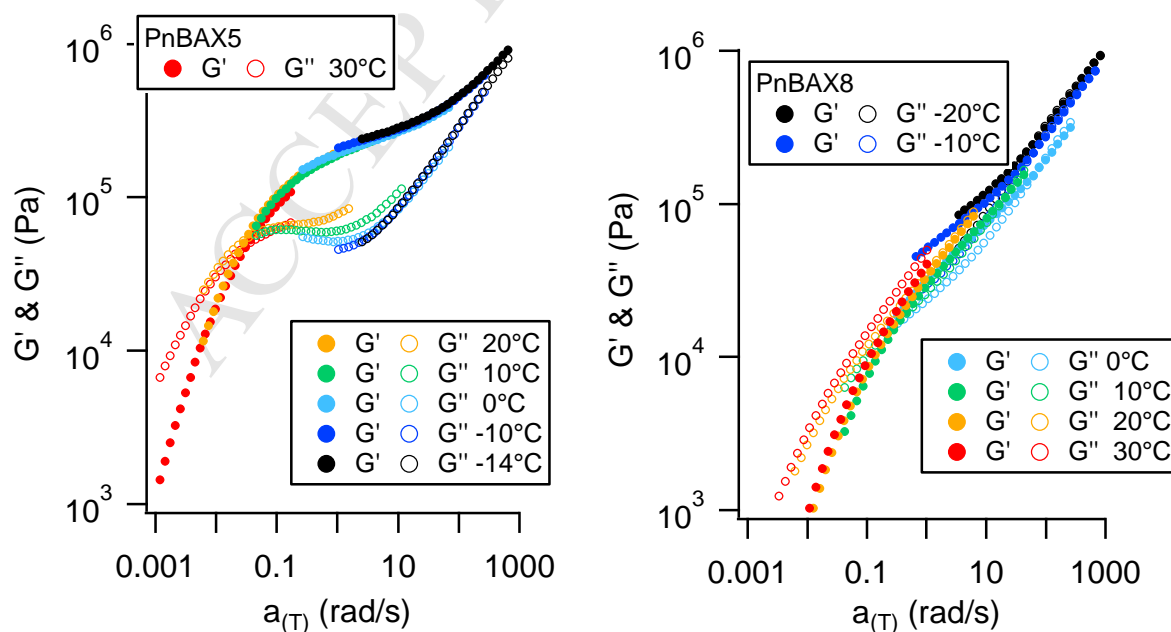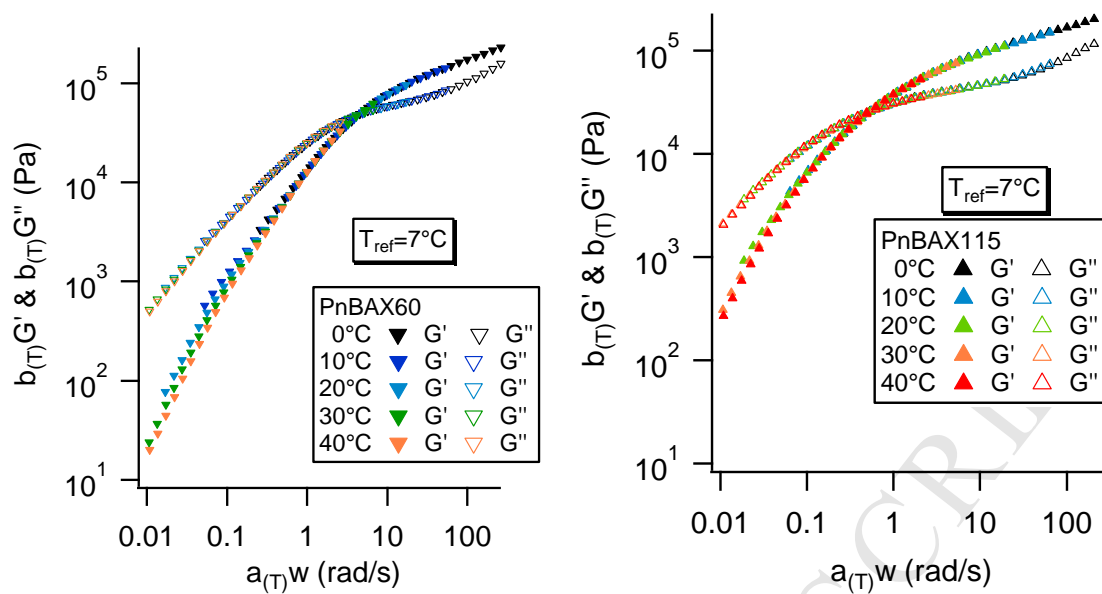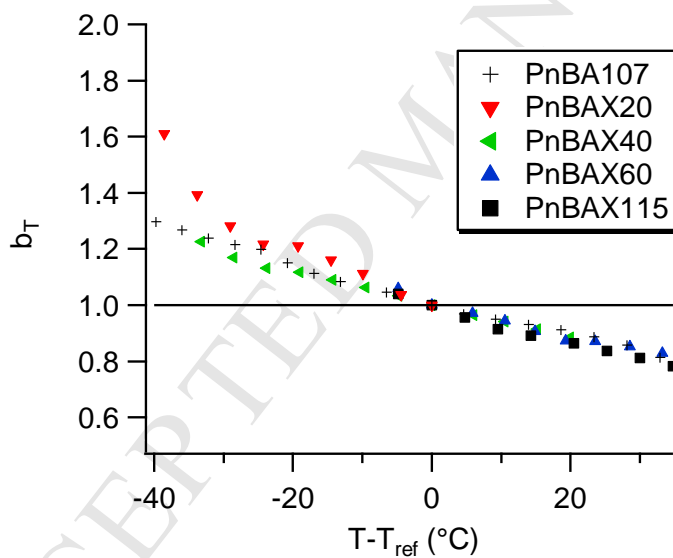Figure S7: Attempts of construction of Master Curves for PnBAX5 and PnBAX8 at $T_{ref} = 7°C$

Figure S8: Master Curves for PnBAX60 and PnBAX115 at $T_{ref} = 7°C$

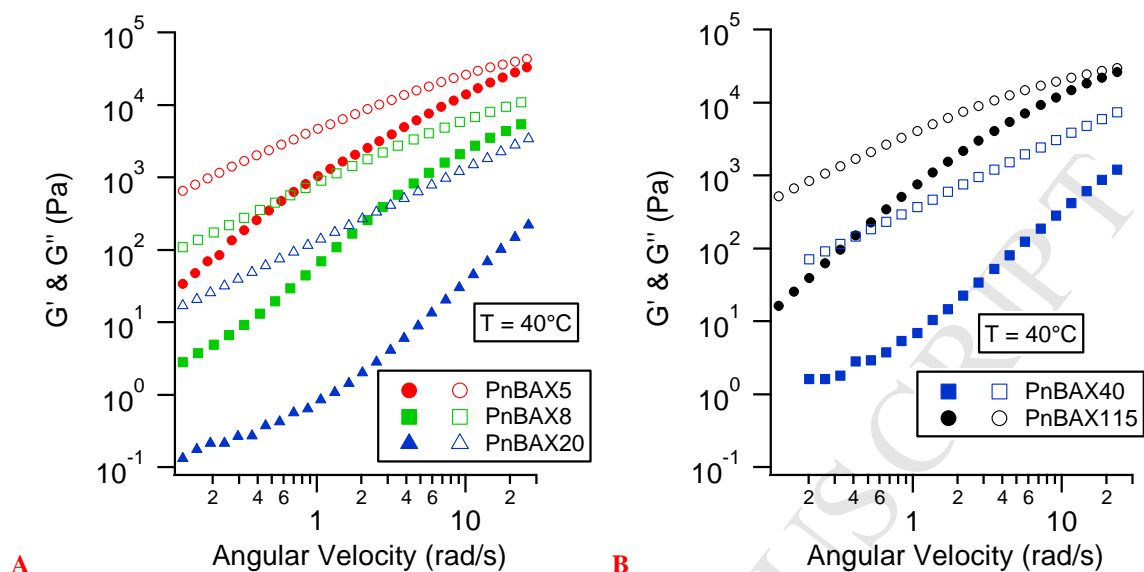Figure S9: Vertical Shifts $b_{(T)}$ for $M_w \geq 20 kg/mol$

7. G' and G'' frequency dependence at 40°C for PnBAXs

Fig S10: Frequency Sweeps for PnBAX systems, in the linear regime at 40°C (A&B). Filled markers represent G' and unfilled markers represent G''.

Materials	Power Scaling Exponent at low frequency (T=40°C)	
	G'	G''
PnBAX5	1,8	1,0
PnBAX8	1,7	1,0
PnBAX20	1,7	1,0
PnBAX40	1,8	0,98
PnBAX60	1,7	1,0
PnBAX115	1,9	1,0
PnBA107	1,7	0,97

Figure S11: Power scaling exponent measured at low frequency for PnBAX polymers. The exponent is obtained by fitting the low frequency end of the data with a power-law of the type $G', G'' = a\omega^n$

8. Numerical model for Linear Unfunctionalized Poly(butylacrylate)

8.1 Molecular Processes for Linear Entangled Polymer Chains

An extensive experimental and numerical study on linear polydisperse PnBA chains was recently published by Jullian et al[1]. In their model[2], the relaxation modulus can be considered as the sum of four molecular processes, A, B, C and D for $M_w \geq 2M_e$.

$$G(t) = G_A(t) + G_B(t) + G_C(t) + G_D(t) \quad (S1)$$

$G(t)$ is measured in a stress relaxation experiment. In our study, the relaxation spectrum $G^*(\omega)$ was determined by strain controlled shear experiments. Thanks to the Fourier transform linearity, $G^*(\omega)$ can be written as follows:

$$G^*(\omega) = G^*_A(t) + G^*_B(t) + G^*_c(t) + G^*_D(t) \quad (S2)$$

As $G^*(\omega) = G'(\omega) + iG''(\omega)$, with the storage modulus G' and the viscous modulus G'' :

$$G'(\omega) = G'_A(\omega) + G'_B(\omega) + G'_c(\omega) + G'_D(\omega) \quad (S3)$$

$$G''(\omega) = G''_A(\omega) + G''_B(\omega) + G''_c(\omega) + G''_D(\omega) \quad (S4)$$

In our study, the polydispersity of our polymers is considered low enough to use a rheological model for monodisperse linear chains. This assumption makes the calculation much simpler compared with those in the polydisperse case. The Process A considers the Rouse-like relaxation of monomers between the transient cross-linking points, called "entanglements ". The maximal characteristic time of this process is the characteristic time τ_a with $\tau_a = \tau_0 N_e^2/6$. τ_0 is the monomer characteristic time and N_e the average number of monomers between two entanglements, $N_e = M_e/m_0$ with M_e the entanglement molecular weight and m_0 the monomer molecular weight. For the butyl acrylate, $m_0 = 128 g/mol$.

Relaxation modulus : $G_A(t) = G^0_N \sum_{p=1}^{Ne} \exp(-tp^2/\tau a)$ (S5)

$$G'_A(\omega) = G^0_N \sum_{p=1}^{Ne} \frac{(\omega\tau)^2}{1+(\omega\tau)^2} \quad (S6)$$

$$G''_A(\omega) = G^0_N \sum_{p=1}^{Ne} \frac{(\omega\tau)}{1+(\omega\tau)^2} \quad (S7) \quad avec \; \tau = \tau_a/p^2$$

The process B considers a Rouse-like diffusion of the entanglement segment through the reptation tube[3].

Relaxation modulus $G_B(t) = (G^0_N/N) \sum_{p=1}^{N} \exp(-tp^2/\tau b)$ (S8)

$$G'_B(\omega) = (G^0_N/N) \sum_{p=1}^{N} \frac{(\omega\tau)^2}{1+(\omega\tau)^2} \quad (S9)$$

$$G''_B(\omega) = (G^0_N/N) \sum_{p=1}^{N} \frac{(\omega\tau)}{1+(\omega\tau)^2} \quad (S10) \quad \text{avec } \tau = \tau b/p^2$$

With N, the number of entanglements segments, $N=M/M_e$ and the characteristic time $\tau_b = \tau_a/2$.

The process C is the reptation diffusion of the polymer chain through its tube. The following equation uses the development brought by Doi[4] by considering the tube length fluctuation.

$$\text{Relaxation module } G_C(t) = G^0_N \int_0^1 \exp\left(-\frac{t}{\tau\xi}\right) d\xi \quad (S11)$$

$$G'_C(\omega) = G^0_N \int_0^1 \frac{(\omega\tau)^2}{1+(\omega\tau)^2} d\xi \quad (S12)$$

$$G''_C(\omega) = G^0_N \int_0^1 \frac{(\omega\tau)}{1+(\omega\tau)^2} d\xi \quad (S13)$$

$$\tau_\xi = \tau_C N\xi^4/(16v^2) \text{ for } 0 < \xi < 2v/\sqrt{N} \quad (S14)$$

$$\tau_\xi = \tau_C (\xi - v/\sqrt{N})^2 \text{ for } 2v/\sqrt{N} < \xi < 1 \quad (S15)$$

τ_C is the characteristic time of the reptation diffusion[5,6,,7] :

$$\tau_C = (\tau_0 N_0^3/N_e) * \left(\frac{1}{1+\frac{M^{0,5}}{15\,N^2}}\right) \quad (S16)$$

According the study done by Majesté[7] between the transition between unentangled and entangled regimes, the adjustable parameter[8,9,10] v equals to 0,5. The process D represents the molecular dynamics at the glass transition. It is modeled by a Davidson-Cole relaxation with three adjustable parameters, the glass modulus G_{glass}, a characteristic time τ_{hf} and a power exponent β.

$$G^*_D(\omega) = G_{glass}(1-(1+j\omega\tau_{hf})^{-\beta}) \quad (S17)$$

<u>8.2 Molecular Processes for Linear Unentangled Polymer Chains</u>

Below the average molecular weight between entanglements M_e, the relaxation of the linear polymer chains is usually described by the Rouse model. The terminal time of the polymer is τ_r with $\tau_{r=}\tau_0 N_0^2/6$ with N_0 the number of monomers in the chain $N_0=M/m_0$. The modulus $G(t)$

can be estimated as the sum of the Rouse-like relaxation G_R t) and a T_g relaxation, i.e. the process D previously described.

$$G(t) = G_R(t) + G_D(t) \quad (S18)$$

$$\text{With } G_R(t) = G^0_R \sum_{p=1}^{Ne} \exp\left(-tp^2/\tau a\right) \quad (S19)$$

After the Fourier transform, $G'_R(\omega) = G^0_R \sum_{p=1}^{N0} \frac{(\omega\tau)^2}{1+(\omega\tau)^2}$ (S20)

$$G''_R(\omega) = G^0_R \sum_{p=1}^{N0} \frac{(\omega\tau)}{1+(\omega\tau)^2} \quad (S21) \text{ avec } \tau = \tau_R/p^2$$

The modulus in the Rouse model is proportional to the density ρ of the polymer but inversely proportional to its molecular weight M_w.

$$G^0_R = \rho RT/M_w \quad (S22)$$

8.3 Transition Rouse regime / Entanglement Regime

Between M_e and $2M_e$, the polymers chains are lightly entangled and their molecular dynamics is highly influenced by the Rouse-like relaxations at short time scales. In order to fit the experimental curves in this M_w range, Majesté and coworkers[7] proposed to suppress the process B and to replace the process A by a Rouse-like relaxation R on the entire chain. Consequently for this M_w range, the authors proposed :

$$G^*(\omega) = G_R^*(\omega) + G_C^*(\omega) + G_D^*(\omega) \quad (23)$$

These equations were successfully used to fit the viscoelastic moduli measured on linear polystyrene chains[7].

8.4. Adjustment of Parameters with experiments

The master curve of the reference synthesized PnBA (M_w=107kg/mol, Ip=1.4) was used to determine the parameters of the viscoelastic model displayed in part 6.1. As the characteristic times τ_0 and τ_{hf} depend only on the nature of monomer, we decided to keep the same values found by Jullian et al[1]. Consequently the molecular weight between entanglements M_e and the modulus G^0_N were adjusted to fit the experimental measurements, as shown in Figure S12 and S13. These parameters were compared with those calculated by Jullian et al in figure S14.

We found a molecular weight between entanglements M_e = 29kg/mol slightly higher for our material than in the reference publication (M_e = 23kg/mol). The difference with the value could be due to the chains polydispersity, i.e. the presence of shorter chains in our reference

sample. Oligomers or small molecules are known to play the role of plasticizers that facilitates the chains diffusion. The main consequences on the rheological properties are the decrease of the viscosity and the characteristic time of the overall material and thus, are similar to those resulted from an Me increase for a fixed molecular weight. The inclusion of polydispersity in the Jullian et al's study explains their low value for Me.

The value obtained for the modulus $G^0_N = 50$kPa is also slightly lower in our work than in the reference study ($G^0_N = 78$kPa). The sensitivity of the rheometer may be at the origin of the slight difference.
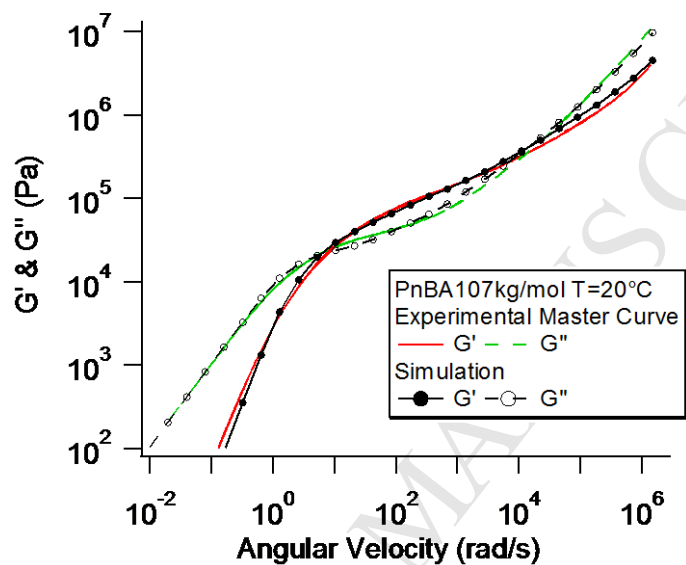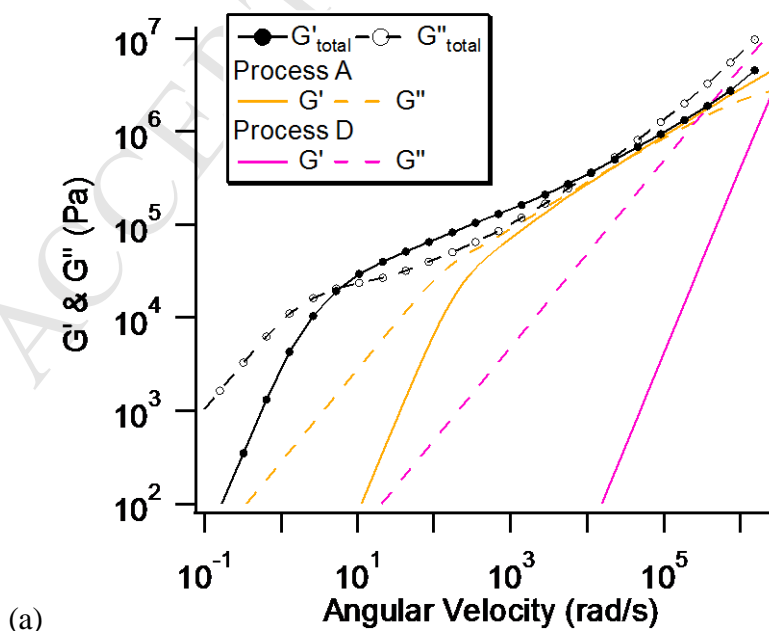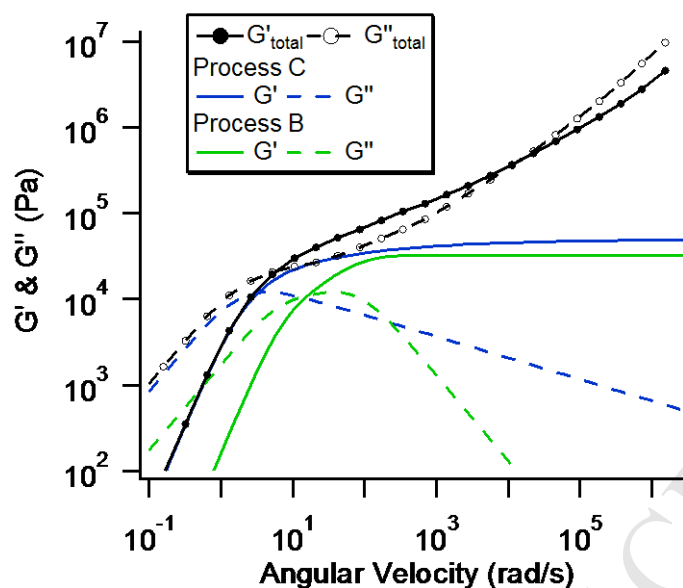
Figure S12: G' & G'' master curve at 20°C compared with the numerical fit from our viscoelastic model.

(a)

(b)

Figure S13: Contributions of the different processes o the G' and G'' curves of PnBA107.

Parameters	Our study	Jullian et al.
G^0_N	50 000 Pa	78 000 Pa
Me	29 kg/mol	23 kg/mol
τ_0	5.10^{-7} s	5.10^{-7} s
τ_{hf}	$1,5.10^{-7}$s	$1,5.10^{-7}$s
G_{glass}	$2.5.10^8$ Pa	No shown
β	0,13	0,13

Figure S14: Parameters of the viscoelastic model for the fit of the master curves of PnBA107 at 20°C.

8.5. Prediction of the G' and G'' curves of linear PnBA chains at different M_w

In the previous section, the fit of the experimental measurements of PnBA107 was used to determine M_e and G^0_N and thus, to predict the viscoelastic moduli G' and G'' for linear unfunc-tionalized PnBA for $M_w \geq 2M_e$ =2*29=58kg/mol. For $Mw \leq 2M_e$ G^0_R (M_w) was adjusted by assuming that the equations (S2) and (S23) must be equivalent for $M_w = 2M_e$, i.e. at the transition between the Rouse regime and the reptation regime. As shown in Figure S15, the equation (S23) with G^0_R = 29kPa gives similar viscoelastic moduli over a large experimental frequency range than the equation (S1). This modulus is a little bit lower than the one obtained by equation (S22):

If T=293K and ρ_{PNBA} =1030kg/m^3 [(1)], G^0_R ($M_w = 2M_e$)=43kPa.
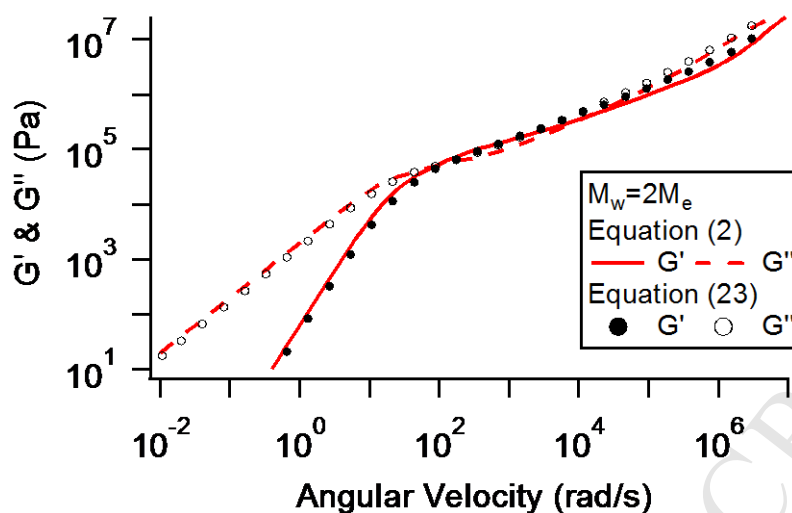
Figure S15: G'' and G' curves for $M_w = 2M_e$ determined by equation (S2) (lines) and equation (S23) (markers).
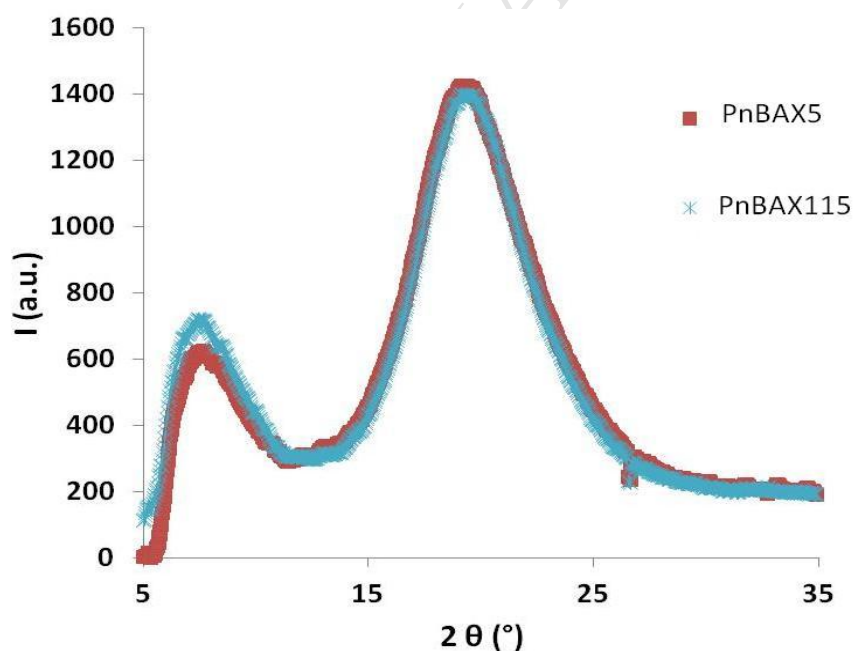
9. Wide Angle X-ray Scattering (WAXS)

Figure S16: X-ray Scattering Spectrum (WAXS) for PnBAX5 and PnBAX115 at room temperature

The self-assembly of stickers in PnBAX was also probed by X-ray scattering at room temperature on a device equipped with a copper rotating anode ($\lambda = 1.54$ Å) (Rigaku Corporation, Tokyo, Japan), a Gobel's mirrors collimation system (ELEXIENCE, Verrières le Buisson, France) and a two-dimensional detector (Princeton Instrument SCX2D, Trenton, NJ,

USA). For WAXS experiments the distance between sample and detector is set at 45 mm and for SAXS experiments the distance is equal to 550 mm. The exposure time is set at 300 seconds. All samples are placed between two thin kapton films to prevent flow. For all patterns the kapton signal is subtracted.

At small angles, no peak was observed and thus, no structuration at long distance range [10nm-4µm] was detected. At wide angles, the two characteristic peaks of the Van der Waals interactions between butylacrylate monomers[11,12] are only observed. (see Figure S16).

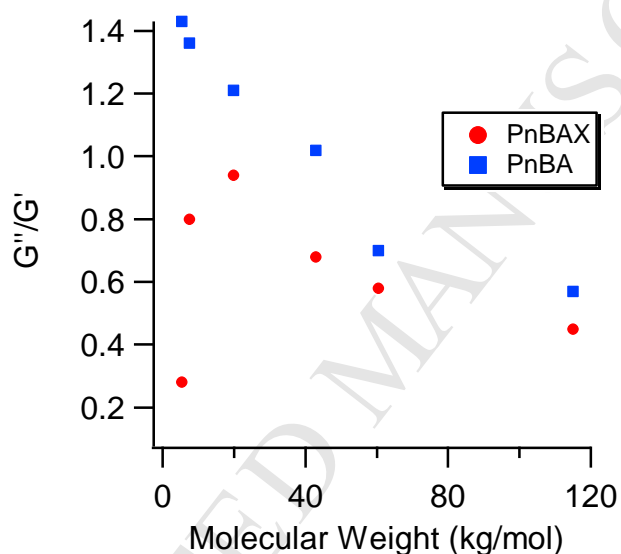## 10. Comparison of Viscoelastic Properties between PnBAX and PnBA

Figure S17: Minimum of $\tan \delta(\omega)$ at $T_{ref} = 7°C$

References

1. Jullian, N., Leonardi, F., Grassl, B., Peyrelasse, J. & Derail, C. Rheological Characterization and Molecular Modeling of Poly (n-Butyl Acrylate). *Appl. Rheol.* **20,** 33685 (2010).

2. Léonardi, F., Majesté, J.-C., Allal, A. & Marin, G. Rheological models based on the double reptation mixing rule: The effects of a polydisperse environment. *J. Rheol.* **44,** 675 (2000).

3. Viovy, J. Tube Relaxation - a Quantitative Molecular-Model for the Viscoelastic Plateau of Entangled Polymeric Media. *J. Polym. Sci. Part B -Polym. Phys.* **23,** 2423–2442 (1985).

4. Doi, M. Explanation for the 3.4 Power Law of Viscosity of Polymeric Liquids on the Basis of the Tube Model. *J. Polym. Sci. Part C-Polym. Lett.* **19,** 265–273 (1981).

5. Daoud, M. & Degennes, P. Some Remarks on the Dynamics of Polymer Melts. *J. Polym. Sci. Part B-Polym. Phys.* **17,** 1971–1981 (1979).

6. Cassagnau, P., Montfort, J. P., Marin, G. & Monge, P. Rheology of polydisperse polymers: relationship between intermolecular interactions and molecular weight distribution. *Rheol. Acta* **32,** 156–167 (1993).

7. Majeste, J. C., Montfort, J. P., Allal, A. & Marin, G. Viscoelasticity of low molecular weight polymers and the transition to the entangled regime. *Rheol. Acta* **37,** 486–499 (1998).

8. Doi, M. & Edwards, S. F. Dynamics of concentrated polymer systems. Part 1.—Brownian motion in the equilibrium state. *J. Chem. Soc. Faraday Trans. 2 Mol. Chem. Phys.* **74,** 1789–1801 (1978).

9. Doi, M. & Edwards, S. d. Dynamics of concentrated polymer systems. Part 2.—Molecular motion under flow. *J. Chem. Soc. Faraday Trans. 2 Mol. Chem. Phys.* **74,** 1802–1817 (1978).

10. Doi, M. & Edwards, S. F. Dynamics of concentrated polymer systems. Part 3.—The constitutive equation. *J. Chem. Soc. Faraday Trans. 2 Mol. Chem. Phys.* **74,** 1818–1832 (1978).

11. Cheng, S., Zhang, M., Dixit, N., Moore, R. B. & Long, T. E. Nucleobase Self-Assembly in Supramolecular Adhesives. *Macromolecules* **45,** 805–812 (2012).

12. Miller, R. L., Boyer, R. F. & Heijboer, J. X-ray scattering from amorphous acrylate and methacrylate polymers: Evidence of local order. *J. Polym. Sci. Polym. Phys. Ed.* **22,** 2021–2041 (1984).